SUPPLEMENTARY INFORMATION

Integrated Iontophoresis and Sweat Sensing via Paper-Derived Laser-Induced Graphene Soft Conductors

Tomás Pinheiro [1,*], Henrique Vazão de Almeida [1], Daniela Nunes [1], Rodrigo Martins [1], Elvira Fortunato [1, *]

[1] CENIMAT|i3N, Departamento de Ciência de Materiais, Faculdade de Ciências e Tecnologia, Universidade Nova de Lisboa and CEMOP/UNINOVA, Campus da Caparica, 2829-516 Caparica – Portugal

[*] tp.pinheiro@campus.fct.unl.pt, emf@fct.unl.pt

1. EXPERIMENTAL SECTION

1.1 Reagents and Materials

During this work, ultrapure Milli-Q water laboratory grade (conductivity < 0.1 $\mu S.cm^{-1}$) was used to prepare all solutions. Sodium tetraborate decahydrate ($Na_2B_4O_7$ $10H_2O$), potassium chloride (KCl), chroroplatinic acid hexahydrate (H_2PtCl_6 $6H_2O$), sulfuric acid (H_2SO_4), agarose, n-(3-Dimethylaminopropyl)-N'ethylcarbodiimide hydrochloride (EDC), n-hydroxi-succinimide (NHS), glucose oxidase (GOx, 158526 units/g), phosphate buffer powder and D-glucose were purchased from Sigma. Carbamylcholine chloride (carbachol) was purchased from Thermo Fisher Scientific. Sodium chloride was purchased from ITW Reagents. All reagents were used as received, without further purification. Whatman chromatography paper grade 1 (Whatman International Ltd., Floram Park, NJ, USA) was used for laser irradiation and LIG formation. Leukoplast Fixomull transparent medical grade polyurethane (PU) tape was used as LIG transfer substrate. For silver track patterning and reference electrode patterning, silver conductive ink (AG-510 silver ink, surface resistivity: <0015 Ω/square/mil, Conductive Compounds, Inc., Hudson, NH) and silver/silver chloride (Ag/AgCl) ink (AGCL-675, Conductive Compounds, Inc., Hudson, NH) were used.

1.2 LIG synthesis and characterization

A CO_2 laser system (VLS 3.50, Universal Laser Systems) with a 10.6 µm wavelength, beam diameter at focus of 0.127 mm, maximum power of 50 W and maximum engraving speed of 1270 $mm.s^{-1}$ was used. For LIG synthesis on paper, substrates were pre-treated with sodium tetraborate and 4 wax layers, as previously reported by our group [1]. After treatment, two LIG engraving cycles were performed with a laser power of 6 W and an engraving speed of 152.4 $mm.s^{-1}$, with a negative beam defocus of 0.79 mm. After paper-derived LIG synthesis, water-induced peel-off transfer was performed [1], by interfacing the adhesive polyurethane medical grade tape with water and gently sticking the paper substrate to the humid surface. After applying slight pressure, peeling-off of the paper substrate is performed, resulting in LIG pattern transfer. Raman characterization was using a Renishaw inVia Reflex micro-Raman spectrometer equipped with an air-cooled CCD detector and a HeNe laser. The laser beam was focused through a 50x Olympus objective lens. Measurements were performed with a 532 nm laser, to perform Raman signal mapping over sample surfaces. Electrical characterization of samples was performed using a 4-point probe Biorad HL 5500 equipment at room temperature. SEM characterization was performed using a Hitachi Regulus SU8220 system. Bright-field (BF) Transmission electron microscopy (TEM) and Scanning Transmission Electron Microscopy (STEM) observations were conducted using a Hitachi HF5000 probe-corrected field-emission transmission electron microscope operating at 80 and 200 kV. Paper-based LIG was extracted from the paper substrate and dispersed in

ethanol. The sonicated dispersion was applied to lacey-carbon copper grids and left to dry prior to observation.

1.3 Fabrication, assembly and testing of iontophoresis device

Two design configurations were developed for the iontophoresis module, the first one to perform sweat secretion rate and volume analysis and the second one for integration with electrochemical sensing modules. Two electrodes with 0.6 cm^2 area were fabricated, to serve as anode and cathode. Subsequently, the electrodes were transferred to the PU substrate, followed by patterning of silver serpentine tracks, using glassine paper masks processed by laser cutting. For the first device configuration, the transfer substrate was also laser cut with an opening, to access and collect iontophoresis-stimulated sweat for analysis. After transfer, the silver tracks were encapsulated with another layer of PU adhesive tape with electrode openings. For the second device configuration, three additional layers were attached above the electrode layer. The first encapsulation layer was a PET substrate, with laser cut electrode openings. This layer was additionally treated with UV ozone lamp for 1 hour, to promote hydrophilicity within the microfluidic network. The second layer was made from a double-sided flexible adhesive (3M 468MP), laser cut with electrode openings and a microfluidic network. The final layer was made from the same PET substrate and double-sided adhesive, laser cut with electrode openings and a sweat accumulation layer, serving to encapsulate the microfluidic layer and attach the device to the skin surface.

After device assembly, agarose hydrogels containing the cholinergic agent were produced. Agarose was dispersed in deionized water to make 3 % w/v concentration, followed by heating the mixture in a microwave for 1 minute, until agarose was dissolved. The mixture was placed on a hotplate, to keep the solution heated. For the anode hydrogel, carbachol was added to a concentration of 0.5 % (w/v). For the cathode hydrogel, NaCl was added to the same concentration. Finally, the mixture was cast onto a glass mold (8x8 cm) and left for gelation at 4 ºC. Hydrogel pads were then laser cut to the shape of the electrodes and placed in the device. Prior to device mounting on the skin, ethanol was used to clean the skin surface of any contaminants. To perform iontophoresis carbachol delivery, varying currents (100 - 450 µA) were applied between the anode and cathode, using a PalmSens4 potentiostat and chronopotentiometry technique, for a period of 10 minutes. For sweat rate and volume estimation, the gravimetric method was employed [2], in which an absorbing chromatography paper pad was used to collect the stimulated sweat, and weighted to determine sweat rate, using the following equation:

$$Rate\ (\mu L.min^{-1}) = \frac{\Delta w\ (g) * 10^3\ \mu L.g^{-1}}{t(min)}$$, *Δw - weight difference of sweat collection pad* (7.3)

1.4 Fabrication and integration of sweat glucose sensor

Using transferred LIG three electrode planar cells on PU substrate, the working electrode was modified to reach high sensitivity to glucose. Firstly, PtNPs were electrodeposited, through cyclic voltammetry, by scanning a potential window between -0.2 and 0.7 V at 50 $mV.s^{-1}$ for 15 cycles, using a 2.5 mM platinum salt solution in 60 mM H_2SO_4. After electrodeposition, the electrode surface was activated though EDC/NHS coupling, for covalent attachment of enzymes. 20 µL of 10 mM EDC and 20 mM NHS mixture was drop-casted onto the electrode surface and incubated at room temperature for 4 hours. After this, the electrode was dried and 10 µL of a 10 $mg.mL^{-1}$ GOx solution in PBS was drop-coated onto the electrode, followed by drying at 4 ºC overnight. Finally, 0.5 % (w/v) agarose hydrogel was prepared as previously presented, and 10 µL were drop-coated over the electrode surface, followed by drying at 4 ºC overnight. For testing, sensors were placed in a beaker with 100 mL electrolyte solution with a magnetic stirrer at 150 rpm. Chronoamperometry was performed for continuous current analysis, using a 0.5 V applied potential, to track current changes by pipetting specific volumes of a stock glucose

solution (100 mM) dissolved in the same electrolyte. Interference analysis was performed by comparing sensor response with PBS buffer against commercial artificial eccrine sweat (Pickering Laboratories, 1700-0020), containing several metabolites (lactic acid, urea, uric acid, ammonia), minerals and amino acids with physiological concentrations.

Glucose sensor integration with the iontophoresis module was made by placing and aligning a functionalized sensor between the iontophoresis electrode layer and the PET encapsulation layer, when assembling the iontophoresis module, using a modular approach. For this case, the PET layer contains a laser cut opening so that flowing sweat can interact with the electrochemical sensor. For device testing, a stimulation cycle was performed, followed by a chronoamperometry measure (0.5 V) of sensor current, to take the signal associated with the fasted state. After a high-calory meal, the same stimulation protocol was performed, to retrieve fresh sweat, followed by chronoamperometry current measurement.

2. Supporting Figures and Tables

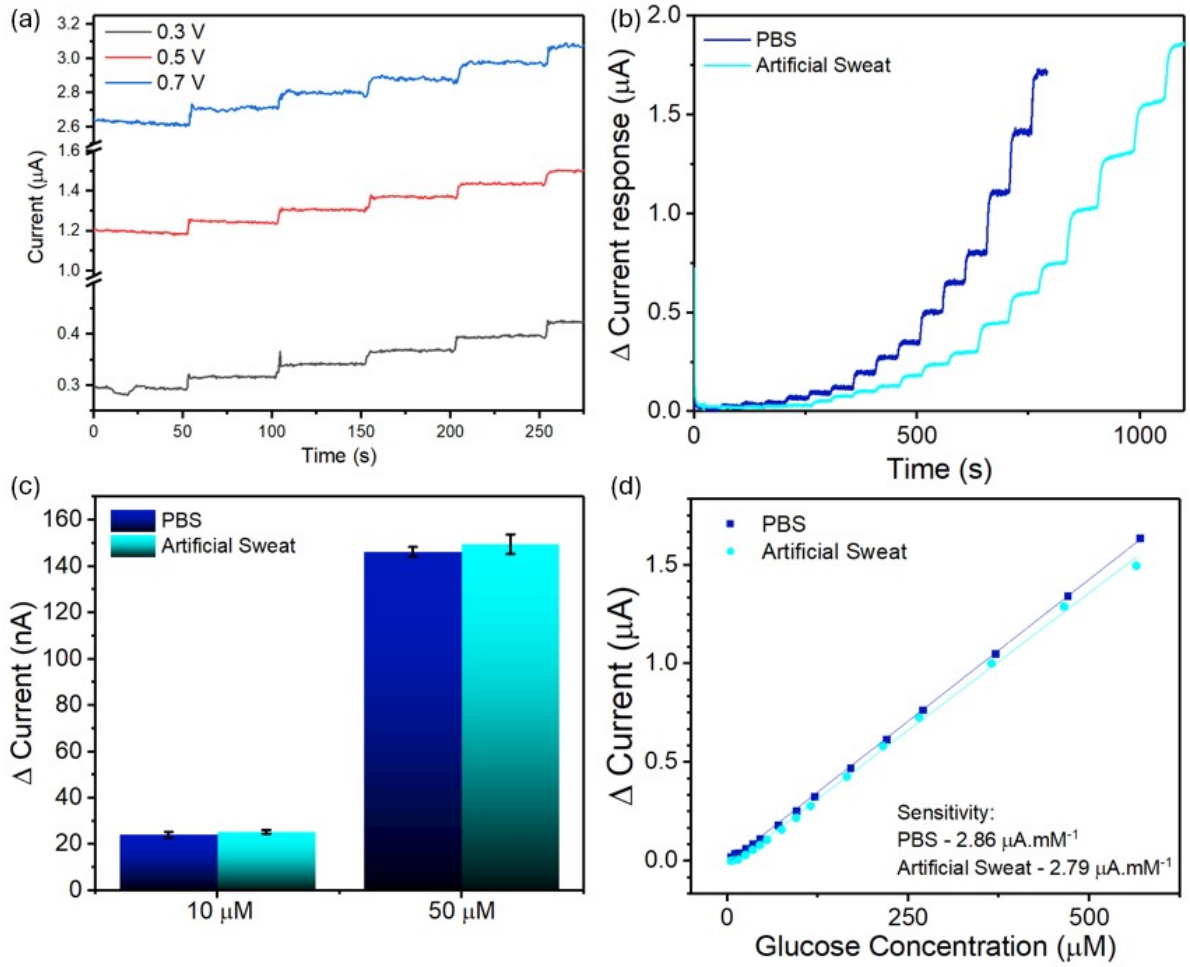

Figure S1 -Enzymatic glucose sweat biosensor testing. (a) Testing of device response for different potential biases, by consecutive addition of 100 μM glucose. Comparative sensors response curves using PBS and commercial artificial sweat, for interference analysis. (c) Comparison of response magnitudes for 10 and 50 μM additions. (d) Comparative calibration curves for full sensor response with PBS and artificial sweat.

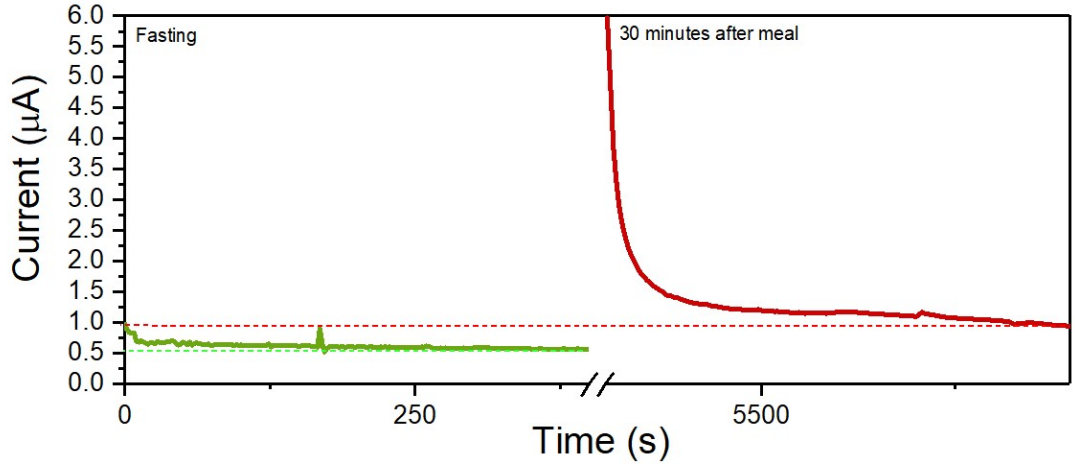

Figure S2 -Sweat glucose detection protocol for a second iontophoresis/sweat glucose sensor integrated device. Although an increase in sensor current is detected after a meal, the current level at a fasted state falls below the minimum values achieved for the calibration curve. This sensor was taken from a different fabrication batch, indicating that more investigation on sensor response and

calibration are needed. In-device integration strategies that monitor pH, temperature, electrolyte levels or other factors may be needed in future investigations for more robust detection.

Table S1. Comparison of skin-interfaced iontophoretic sweat stimulation devices and resulting sweat stimulation capabilities.

Electrode material	Cholinergic agonist (w/v %)	Iontophoresis current (mA)	Stimulation time (min)	Generated Sweat rate/volume	Reference
Ag/AgCl	Pilocarpine (1 %)	0.6	5	-	[3]
Gold	Acetylcholine (10%)	2	5	0.354 $\mu L.min.cm^{-2}$	[4]
	Methacholine (10%)	2	5	0.252 $\mu L.min.cm^{-2}$	
	Pilocarpine (10%)	2	5	0.210 $\mu L.min.cm^{-2}$	
Carbon	Carbachol (1%)	0.28 ($mA.cm^{-2}$)	3	0.320 $\mu L.min^{-1}$	[5]
Gold	Pilocarpine (1%)	0.6	5	0.07 $\mu L.mm^{-2}$	[6]
Ag/AgCl	Pilocarpine (2%)	0.3 ($mA.cm^{-2}$)	10	-	[7]
Ag/AgCl	Pilocarpine (2%)	0.4 ($mA.cm^{-2}$)	10	2 µL	[8]
LIG@polyimide	Carbachol (1%)	0.1	5	3 $\mu L.min^{-1}$	[9]
Paper-based LIG soft conductor	Carbachol (0.5%)	0.25	10	1 $\mu L.min^{-1}$	This work

References:

(1) Pinheiro, T.; Correia, R.; Morais, M.; Coelho, J.; Fortunato, E.; Sales, M. G. F.; Marques, A. C.; Martins, R. Water Peel-Off Transfer of Electronically Enhanced, Paper-Based Laser-Induced Graphene for Wearable Electronics. *ACS Nano* **2022**, *16* (12), 20633–20646. https://doi.org/10.1021/acsnano.2c07596.

(2) Simmers, P.; Li, S. K.; Kasting, G.; Heikenfeld, J. Prolonged and Localized Sweat Stimulation by Iontophoretic Delivery of the Slowly-Metabolized Cholinergic Agent Carbachol. *J. Dermatol. Sci.* **2018**, *89* (1), 40–51. https://doi.org/10.1016/j.jdermsci.2017.10.013.

(3) Kim, J.; Jeerapan, I.; Imani, S.; Cho, T. N.; Bandodkar, A.; Cinti, S.; Mercier, P. P.; Wang, J. Noninvasive Alcohol Monitoring Using a Wearable Tattoo-Based Iontophoretic-Biosensing System. *ACS Sensors* **2016**, *1* (8), 1011–1019. https://doi.org/10.1021/acssensors.6b00356.

(4) Emaminejad, S.; Gao, W.; Wu, E.; Davies, Z. A.; Nyein, H. Y. Y.; Challa, S.; Ryan, S. P.; Fahad, H. M.; Chen, K.; Shahpar, Z.; Talebi, S.; Milla, C.; Javey, A.; Davis, R. W. Autonomous Sweat Extraction and Analysis Applied to Cystic Fibrosis and Glucose Monitoring Using a Fully Integrated Wearable Platform. *Proc. Natl. Acad. Sci. U. S. A.* **2017**, *114* (18), 4625–4630. https://doi.org/10.1073/pnas.1701740114.

(5) Hauke, A.; Simmers, P.; Ojha, Y. R.; Cameron, B. D.; Ballweg, R.; Zhang, T.; Twine, N.; Brothers, M.; Gomez, E.; Heikenfeld, J. Complete Validation of a Continuous and Blood-Correlated Sweat Biosensing Device with Integrated Sweat Stimulation. *Lab Chip* **2018**, *18* (24), 3750–3759. https://doi.org/10.1039/C8LC01082J.

(6) Hojaiji, H.; Zhao, Y.; Gong, M. C.; Mallajosyula, M.; Tan, J.; Lin, H.; Hojaiji, A. M.; Lin, S.; Milla, C.; Madni, A. M.; Emaminejad, S. An Autonomous Wearable System for Diurnal Sweat Biomarker Data Acquisition. *Lab Chip* **2020**, *20* (24), 4582–4591. https://doi.org/10.1039/D0LC00820F.

(7) Sempionatto, J. R.; Khorshed, A. A.; Ahmed, A.; De Loyola E Silva, A. N.; Barfidokht, A.; Yin, L.; Goud, K. Y.; Mohamed, M. A.; Bailey, E.; May, J.; Aebischer, C.; Chatelle, C.; Wang, J. Epidermal Enzymatic Biosensors for Sweat Vitamin C: Toward Personalized Nutrition. *ACS Sensors* **2020**, *5* (6), 1804–1813. https://doi.org/10.1021/acssensors.0c00604.

(8) Bolat, G.; De la Paz, E.; Azeredo, N. F.; Kartolo, M.; Kim, J.; de Loyola e Silva, A. N.; Rueda, R.; Brown, C.; Angnes, L.; Wang, J.; Sempionatto, J. R. Wearable Soft Electrochemical Microfluidic Device Integrated with Iontophoresis for Sweat Biosensing. *Anal. Bioanal. Chem.* **2022**, *414* (18), 5411–5421. https://doi.org/10.1007/s00216-021-03865-9.

(9) Wang, M.; Yang, Y.; Min, J.; Song, Y.; Tu, J.; Mukasa, D.; Ye, C.; Xu, C.; Heflin, N.; McCune, J. S.; Hsiai, T. K.; Li, Z.; Gao, W. A Wearable Electrochemical Biosensor for the Monitoring of Metabolites and Nutrients. *Nat. Biomed. Eng.* **2022**, *6* (11), 1225–1235. https://doi.org/10.1038/s41551-022-00916-z.